Vol. 86 No. 3 pp. 630–639 ACTA GEOLOGICA SINICA (English Edition) June 2012

Geology and Geochemistry of the Bianbianshan Au-Ag-Cu-Pb-Zn Deposit, Southern Da Hinggan Mountains, Northeastern China

ZENG Qingdong*, LIU Jianming and LIU Hongtao

Key Laboratory of Mineral Resources, Institute of Geology and Geophysics, Chinese Academy of Sciences, Beijing 100029, China

Abstract: The Bianbianshan deposit, the unique gold-polymetal (Au-Ag-Cu-Pb-Zn) veined deposit of the polymetal metallogenic belt of the southern segment of Da Hinggan Mountains mineral province, is located at the southern part of the Hercynian fold belt of the south segment of Da Hinggan Mountains mineral province, NE China. Ores at the Bianbianshan deposit occur within Cretaceous andesite and rhyolite in the form of gold-bearing quartz veins and veinlet groups containing native gold, electrum, pyrite, chalcopyrite, galena and sphalerite. The deposit is hosted by structurally controlled faults associated with intense hydrothermal alteration. The typical alteration assemblage is sericite + chlorite + calcite + quartz, with an inner pyrite - sericite - quartz zone and an outer seicite - chlorite - calcite - epidote zone between orebodies and wall rocks. δ^{34}S values of 17 sulfides from ores changing from –1.67 to +0.49‰ with average of –0.49‰, are similar to δ^{34}S values of magmatic or igneous sulfide sulfur. $^{206}Pb/^{204}Pb$, $^{207}Pb/^{204}Pb$ and $^{208}Pb/^{204}Pb$ data of sulfide from ores range within 17.66–17.75, 15.50–15.60, and 37.64–38.00, respectively. These sulfur and lead isotope compositions imply that ore-forming materials might mainly originate from deep sources. H and O isotope study of quartz from ore-bearing veins indicate a mixed source of deep-seated magmatic water and shallower meteoric water. The ore formations resulted from a combination of hydrothermal fluid mixing and a structural setting favoring gold-polymetal deposition. Fluid mixing was possibly the key factor resulting in Au-Ag-Cu-Pb-Zn deposition in the deposit. The metallogenesis of the Bianbianshan deposit may have a relationship with the Cretaceous volcanic-subvolcanic magmatic activity, and formed during the late stage of the crust thinning of North China.

Key words: Gold-polymetal deposit, isotopes, Da Hinggan Mountains, China

1 Introduction

The Bianbianshan deposit is the unique gold-polymetal deposit discovered in the south segment of Da Hinggan Mountains mineral province (DHMP) in 1971. Geological exploration performed in 1984 under a project of Complex Geological Team of the Metallurgical Industry Ministry. The deposit has been mined since 1996. The geologic and geochemical data on deposit have not been published in journals. Geologic features of the gold deposit were briefly described by Xiao and Yang (1997), and the deposit was thought to be a porphyry type deposit (Xiao and Yang, 1997; Xiao et al., 2000; Wang et al., 2000). The regional geological setting and metallogenesis of south segment of DHMP have been discussed by numerous workers. Accordingly, the south segment of DHMP is a Hecynian accretionary zone of North China plate (Fig. 1) (Rui et al., 1994; Zhao and Zhang, 1997; Xiao et al., 2000; Liu, 2001; Zeng et al., 2010a, 2010b, 2011a, 2011b, 2011c). However, the detailed ore-forming processes, the source of ore-forming fluid and material, and the genetic relation between the gold mineralization and volcanic-subvolcanic activity have not yet been discussed. This paper describes the basic geological and geochemical features of the Bianbianshan deposit. Sulfur, lead, H and O isotope data are reported, with the aim of constraining possible sources of gold-polymetal and ore-forming processes.

* Corresponding author. E-mail: zengqingdong@mail.iggcas.ac.cn

2 Geological Setting

Study area belongs to the Hercynian fold belt of south segment of the Da Hinggan Mountains mineral province

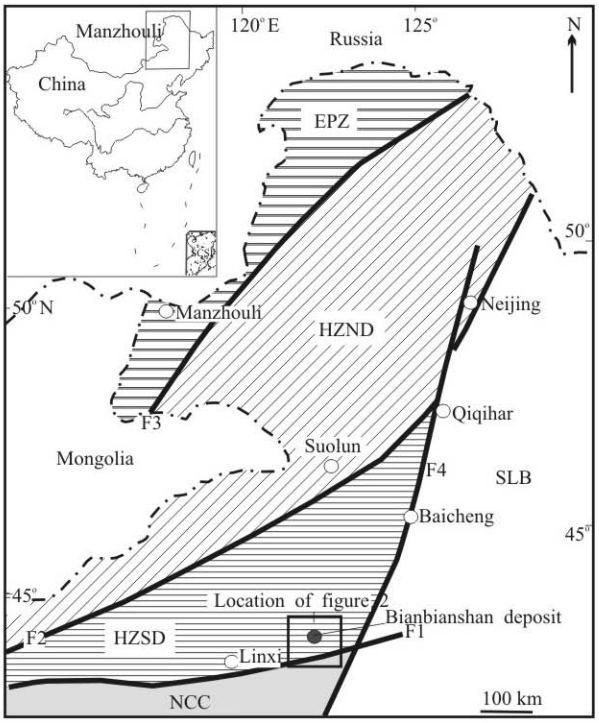

Fig. 1 Structural units of the Da Hinggan Mountains mineral province showing the location of the studied area (modified from BGMR, 1991; Zhao and Zhang, 1997).
EPZ-Erguna fold zone; HZND-Hercynian fold zone of north segment of DHMP; HZSD-Hercynian fold zone of south segment of DHMP; NCC-North China Craton. F1-Xar Moron He Fault; F2-Erlian-Hegenshan Fault; F3-Deerbugan Fault; F4-Neijiang Fault.

(DHMP), northeastern China (Fig. 1). The DHMP is composed of Siberia plate, North China plate and Mesozoic volcanic belt. Siberia and North China plates are bounded by the Erlian-Hegenshan fault (Shao, 1991; BGMR, 1991, 1996; Wu et al., 2010) (Fig. 1). The DHMP is overlain by the Mesozoic volcanics, volcano plutonic and sedimentary rocks of the Da Hinggan Mountains volcanic belt. The DHMP is divided into three main structural belts separated by regional faults: (1) Erguna fold zone, (2) Hercynian fold zone of north segment of the DHMP, (3) Hercynian fold belt of south segment of the DHMP (Fig. 1). The DHMP is divided into three metallogenic belts based on its geological setting: Pb-Zn-Ag-Cu-Sn-Fe-Mo metallogenic belt of the south segment of DHMP, Cu-Mo-Fe –Pb-Zn-Au metallogenic belt of the north segment of DHMP, and Erguna Cu-Pb-Zn-Ag-Mo-Au metallogenic belt (Fig. 1). The typical metal deposits in the three metallogenic belt are described by Zeng et al. (2011a).

The Cretaceous volcanics and volcanic clastic rocks were formed on a basement of Permian marble and metamorphic andesite, tuff, metamorphic sandstone, siltstone and slate. The Cretaceous rocks include rhyolite, dacite, andesite and tuff (Fig. 2).

Some Yanshanian granites, consisting of granite, granodiorite and granite porphyry, occurs as stock (Fig. 2) and dyke. Intrusion such as Haolibao granite porphyry has

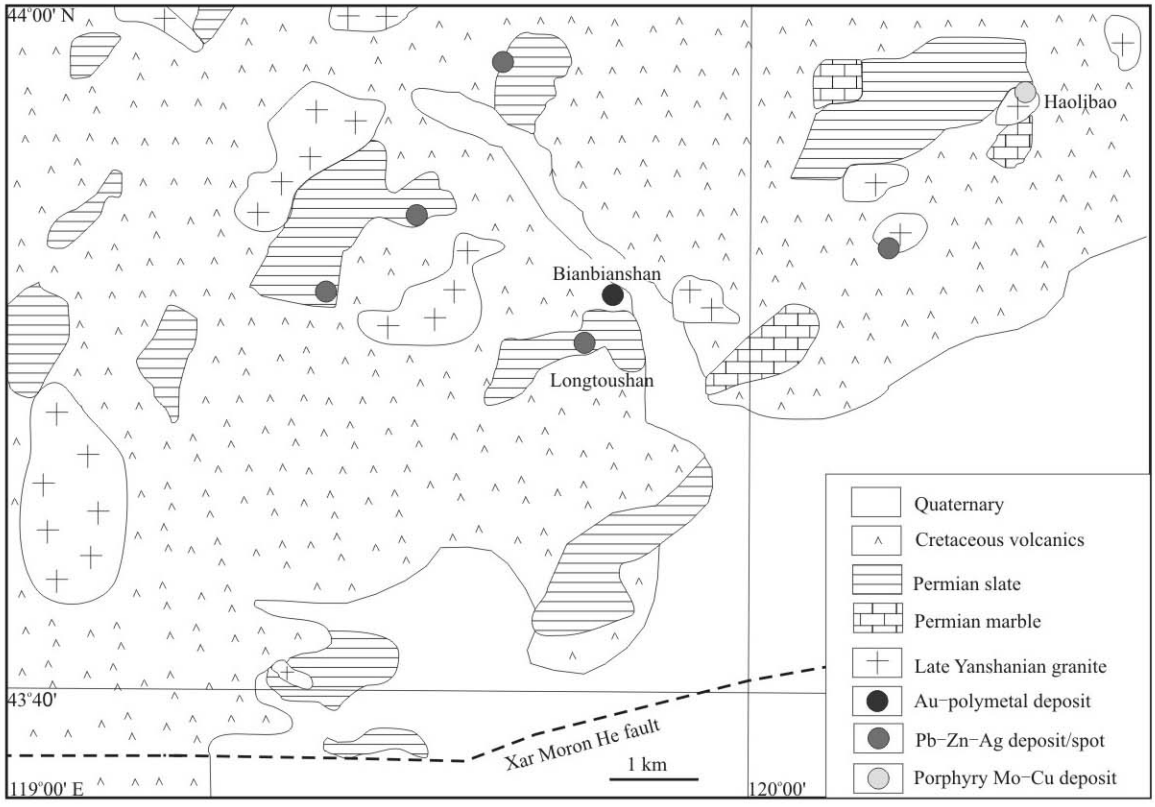

Fig. 2 Regional geology of Bianbianshan deposit.

been dated by K-Ar methods at 113 Ma (Wang et al., 2000). The dyke such as dacite porphyry in Bianbianshan ore area has been dated by K-Ar methods at 109.2 Ma (Zhao et al., 2004).

The metal deposits can be divided into four types, they are: (1) Au-polymetal deposit occurring within the Cretaceous rocks (e.g. Bianbianshan deposit); (2) porphyry Mo-Cu deposit occurring within the granite (e.g. Haolibao deposit) (Zeng et al., 2009a, 2009b); (3) Zn-Pb-Ag deposits occurring within the Permian (e.g. Longtoushan deposit), these deposits are characterized by the following features: A– these deposits have experienced two metallogenic periods including hot-water sedimentation period and hydrothermal reformation period. B-the shape of oreboies are bedded, veined and lense shape (Sun, 2008), and (4) Ag-polymetal deposit occurring within the granodiorite (e. g. Lamahanshan deposit), is controlled by brittle faults and is characterized by Ag, Pb and Zn-bearing quartz veins (Li et al. 2008).

3 Features of the Bianbianshan Deposit

3.1 Host rocks and magmatism

The Bianbianshan deposit is hosted by the late Cretaceous andesite and tuff (Fig. 3). Andesite occurs at the northeast part of the ore area. Tuff occurs at the southwest part of the ore area. These rocks have been strongly altered by chloritization, silicification, sericitization and epidotization.

A dacite porphyry dikes occur within the mineralizing zone, and has been altered by stongly altered by silicification and sericitization, and constitute the wall rocks of ore bodies. The K-Ar age of dacite porphyry rock is 109.2 Ma (Zhao et al., 2004).

3.2 Structures

The EW-trending fault (F1) and NW-trending fault are well developed, and the EW-trending fault is considered as the controlling factor of gold mineralization. The EW-trending fault is a left-hand shear fault, and the dilatation zone of fault controls the distribution of the ore bodies, the main fault dips to northwest with an angle of 75°–80°. The V1 ore body occurs within the main fault, and other ore bodies occur in the secondary fractures (Fig. 3).

The NW-trending fault (F2) is a cataclastic zone, it is 30 m wide and dips to southwest with an angle of 80°–85°. It is a formal fault and cut the ore-bearing fault (Fig. 3). The ore-bearing zone at the hanging wall of the F2 is buried in the depth.

3.3 Ore bodies

Metal mineralization at Bianbianshan is spatially confined to the dilatation zone of an EW-trending fault, with a strike length of 300 m, widths varying from 50 to 100 m, and a down-dip depth in excess of 150 m. Orebodies occur mainly as veins localized in the inner pyrite – sericite – quartz zone, and five ore bodies (V1, V2, V3, V4 and V5) have been defined (Figs. 3, 4). The trend of the veins is northeast-east – southwest-west. The veins are located within the Cretaceous andesite.

The V1 vein branches off two veins at surface in section (Fig. 4). The length of the V1 ore vein is about 220 m,

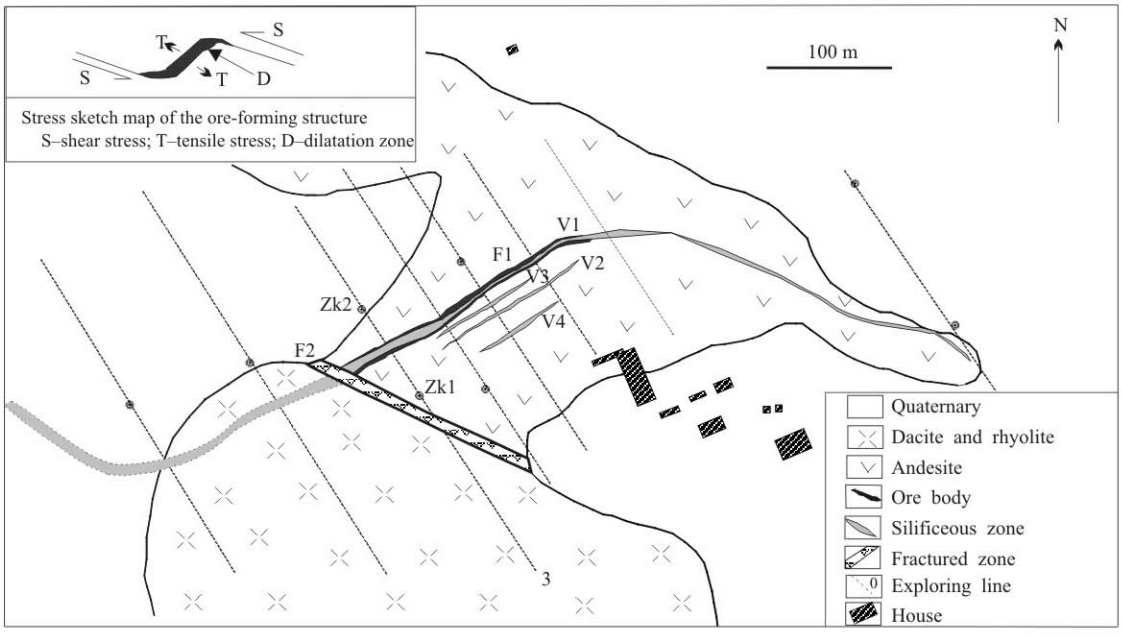

Fig. 3 Geological map of the Bianbianshan deposit.
Modified from the Second Regional Geological Survey Team, Inner Mongolia, written communication, 1982.

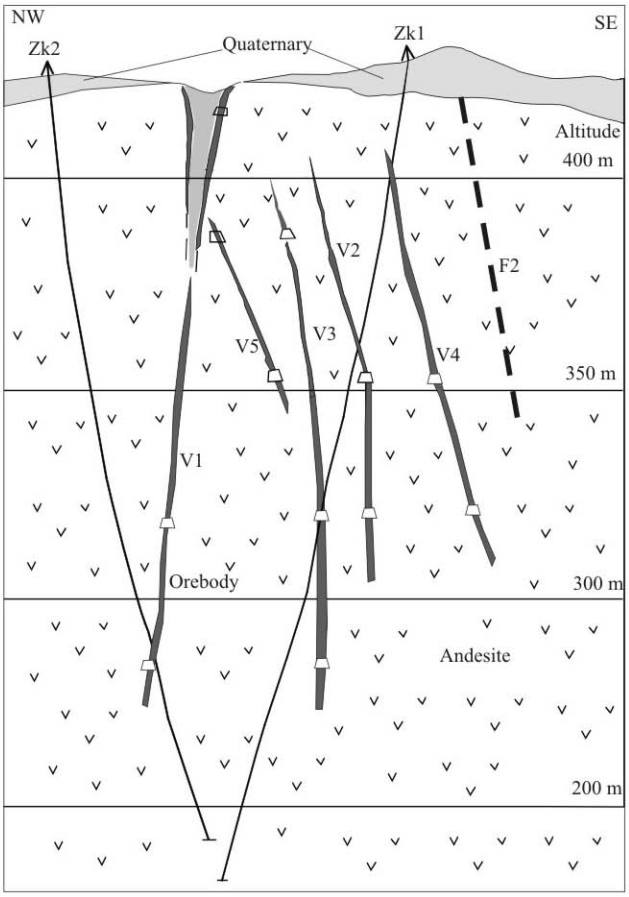

Fig. 4 Geological section across the Bianbianshan deposit. Modified from the Second Regional Geological Survey Team, Inner Mongolia, written communication, 1982. The section line is shown in Fig. 3.

with an average thickness of 1.92 m and a decline depth of 300 m, the ore grade of V1 ore vein is: Au=1.37–9.27 g/t, Ag=20–169 g/t, Cu=1.28%, Pb=0.63% Zn=1.18%. The length of the V2 ore veins is about 200 m, with an average thickness of 1.79 m and a decline depth of 250 m, the ore grade is Au=1.34–5.08 g/t, Ag=15–43 g/t, Cu=2.88%, Zn=15.66%. The length of the V3 ore veins is about 200 m, with an average thickness of 0.66m and a decline depth of 250 m, the ore grade is Au=3.15 g/t, Ag=141 g/t. The length of the V4 ore veins is about 200 m, with an average thickness of 0.89m and a decline depth of 200 m, the ore grade is Au =2.76 g/t, Ag=27 g/t, Cu=1.79%, Zn=8.96%. The ore bodies above 350 m level are Au and Ag riched ore bodies, and the ore bodies under 350 m level are Cu-Pb-Zn –riched ore bodies. Some smaller ore bodies also occur within the dilatation zone (Fig. 3), the length of the ore bodies is generally lesser than 100 m, and with a thickness of 0.7 m.

The common ore consists of large amounts of pyrite, chalcopyrite, sphalerite and galena. They occur as (1) veinlets in dominantly gray-colored quartz, and (2) as band in quartz-polymetal sulfide vein and (3) finally as dissemination in white-colored quartz. Gold minerals are native gold and electrum. Hydrothermal quartzs are the common gangue minerals. Mineralization can be classified into three main stages based on paragenetic sequence: A—grey-colored quartz vein, containing minor disseminated pyrite and chalcopyrite. Analyses indicate that veins contain low gold. Grey-colored vein quartz is typically anhedral and fractured. Both vein quartz and pyrite are commonly fractured and locally cemented by ore– and late ore-stage minerals; B—the gold mineralization stage, consists of white quartz, pyrite, sphalerite and galena. It is characterized by enrichment of the sphalerite and galena. The sulfide vein often crosscuts the early stage minerals. C—Post ore-stage calcite. Coarse translucent euhedral calcite crystals occur in fracture zones, these veinlets crosscut the sulfides and quartz minerals. There are distinct alteration mineral assemblages surrounding the quartz lodes. From orebody to wall rock, three alteration zones are identified: (i) inner zone (phyllic zone), 2–15m wide, with a characteristic mineral assemblage of pyrite + quartz + sericte; (ii) middle zone (sericite zone), 10-20m wide, with a characteristic sericite mineral; and (iii) outer prophylitic zone, 30–50 m wide, with dominant assemblage of chlorite + epidote + carbonate. Contacts among the alteration zones are generally gradational.

4 Features of the Fluid Inclusions

4.1 Method of study

Doubly polished thin sections, approximately 100 μm thick, were prepared from 25 quartz samples for preliminary petrographic study. 11 samples were selected for detailed analysis. The homogenization temperature (Th) was measured for 108 fluid inclusions.

All geothermometric measurements are carried out with a LinKam THMSG600 heating / freezing stage provided with a thermal control unit and equipped with a binocular Nikon microscope with a magnification up to 400. Freezing and heating runs are, respectively, undertaken using liquid nitrogen and a thermal resistor. The lower and upper temperature limits of stage are –198°C and +600°C, respectively. To ensure accurate observation of melting behaviour, heating rates are slow (0.5 to 1°C /min) whilst to avoid metastability, freezing rates are very much faster. The T_m of aqueous inclusions is difficult to monitor and not be measured. In contrast, temperature of homogenization (T_h) for aqueous inclusions is readily observable and can be duplicated within ±0.2°C.

4.2 Occurrence of fluid inclusions and microthermometric results

In the Bianbianshan deposit, some fluid inclusions have

been observed in quartz. In this study, representative samples of the various vein stages from the V1, V2, V3 and V4 ore bodies were selected for fluid inclusion analysis, and the studied fluid inclusions are hosted in quartz. The criteria listed by Roedder (1984) and Roedder and Bodnar (1980) were used to discriminate primary, pseudosecondary and secondary fluid inclusions. Some isolated fluid inclusions were treated as primary. Trails of inclusions along transgranular fractures are obviously secondary. Only primary inclusions were selected for microthermometry. The inclusion size varies but most of that studied fall between 3 to 10 μm. The inclusions are mainly rounded with less columnar inclusions. Two main types of fluid inclusions have been identified at room temperature on the basis of geometry, phases and phase proportions, and composition. They are: type (I) aqueous biphase inclusions: aqueous vapor and an aqueous liquid phase (L+V); type (II) monophase aqueous liquid (Laq.). The distribution characteristics of the two type fluids is that liquid phase inclusions are mainly occur within the quartz in late stage quartz-calcite veins, and two phase vapor and liquid fluid inclusions mainly occur within the gold-polymetal-bearing quartz veins.

Fluid-inclusion homogenization temperatures are shown in Fig. 5. Fig. 5 reveals wide and different ranges of homogenization temperature of primary fluid inclusions in the different stage quartz. It may reflect gold, silver, copper, lead and zinc deposition took place at temperatures of 80°C to 360°C with an wide peak of 220°C–300°C in the Bianbianshan deposit.

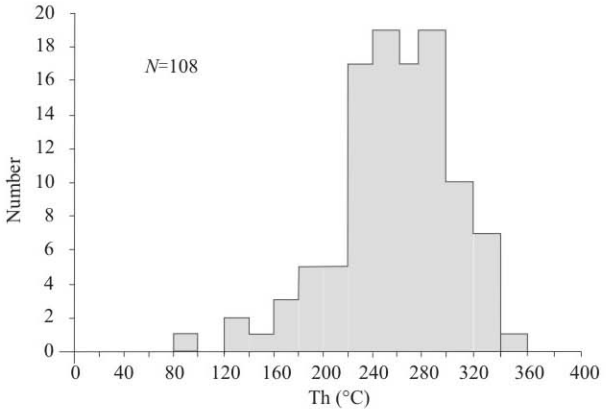

Fig. 5 Histogram of homogenization temperature of the primary fluid inclusions from the Bianbianshan deposit.

4.3 Gas chemistry

The gas compositions of fluid inclusions were analyzed with a rapid-scanning quardrupole mass spectrometer in the laboratory of the Institute of Geology and Geophysics, Chinese Academy of Sciences. The H_2O, CO_2, N_2, CH_4, C_2H_4, H_2S and Ar contents were determined quantitatively by bulk analysis. The "bulk" means the mixture of all the inclusion gases of obtained by decrepitation in the furnace. The results of bulk analysis of ten samples (Table 1) indicate that the inclusion fluids mainly comprise H_2O and CO_2. The concentration of CO_2 ranges from 0.6–1.4 mol%. N_2 is about one order of magnitude less than CO_2. The H_2S content is variable and consistently less than N_2. The Ar, the C_2H_6 and the CH_4 contents in all of the samples are small.

5 Oxygen and Hydrogen Isotopes

The isotopic analysis results of oxygen and hydrogen for ten quartz samples from the main ore-forming stage of the V1, V2 and V4 ore bodies are presented in Table 2. The samples were ground to –60 mesh size. Quartz was hand-picked and/or separated using a magnetic separator. Oxygen was liberated from quartz by reaction with BrF_5 (Clayton and Mayeda, 1963) and converted to CO_2 on a platinum-coated carbon rod. The $\delta^{18}O$ determinations were made on a MAT-252 mass spectrometer. Reproducibility for isotopically homogeneous pure quartz is about ±0.2‰ (1σ).

Analyses of hydrogen isotopic compositions of the inclusion fluids have been made on the ten quartz vein samples. Water was released by heating the samples approximately 500°C in an induction furnace. Samples were first degassed of labile volatiles by heating under vacuum to 120° C for 3 h. Water was converted to hydrogen by passage over heated zinc powder at 410°C and the hydrogen was analyzed with a MAT-252 mass spectrometer. Analysis of standard water samples gives the accuracy of ±2‰ (1σ).

The $\delta^{18}O_{fluid}$ values were calculated from the $\delta^{18}O$ values for quartz and the formation temperatures obtained from fluid inclusions, using an equation for quartz-water

Table 1 Results of bulk analyses of gases in fluid inclusions (gas contents: mol %)

Sample No.	B5-17	B5-16	B5-12	B5-11	B4-16	B4-15	B4-2	B3-11	B3-8	B3-4
H_2O	98.88	98.52	98.34	98.59	98.63	98.84	99.28	97.54	98.28	99.09
N_2	0.150	0.153	0.178	0.132	0.198	0.049	0.015	0.343	0.310	0.225
CO_2	0.878	1.222	1.408	1.195	1.026	0.983	0.602	1.759	1.298	0.589
Ar	0.0039	0.0018	0.0024	0.0048	0.0034	0.0040	0.0045	0.0117	0.0167	0.0159
CH_4	0.0167	0.0094	0.0120	0.0214	0.0193	0.0344	0.0158	0.0414	0.0456	0.0497
C_2H_6	0.0131	0.0067	0.0086	0.0498	0.0115	0.0823	0.0814	0.0145	0.0232	0.0244
H_2S	0.0582	0.0868	0.0515	0.0073	0.1125	0.0075	0.0010	0.2990	0.0260	0.0059

The sample descriptions were seen in Table 2.

Table 2 Hydrogen and oxygen isotope compositions of the quartz from the Bianbianshan deposit

Number	Sample description	Locality	t (°C)	$\delta^{18}O$ (‰)	$\delta^{18}O_{H_2O}$ (‰)	δD (‰)
B3-4	Polymetal sulfides quartz vein	V1, 3level	213	8.93	−1.98	−83
B3-8	Polymetal sulfides quartz vein	V1, 3level	247	9.06	−0.04	−91
B3-11	Polymetal sulfides quartz vein	V1, 3level	249	8.54	−0.46	−83
B4-2	Polymetal sulfides quartz vein	V1, 4level	266	9.08	−0.85	−89
B4-15	Polymetal sulfides quartz vein	V4, 4level	247	8.60	−0.5	−86
B4-16	Polymetal sulfides quartz vein	V4, 4level	242	9.78	−0.44	−96
B5-11	Polymetal sulfides quartz vein	V2, 5level	213	10.28	−0.63	−99
B5-12	Polymetal sulfides quartz vein	V1, 5level	247	8.94	−0.16	−88
B5-16	Polymetal sulfides quartz vein	V4, 5level	247	9.45	0.35	−92
B5-17	Polymetal sulfides quartz vein	V4, 5level	284	9.21	1.71	−91

isotopic equilibrium (Matsuhisa et al., 1979).

The calculated oxygen isotope composition of the fluid varies between 1.71‰ and –1.98‰ (Table 2). The analyses of hydrogen isotopic composition, measured directly on inclusion fluid, gave a relatively narrow spread between –83 and –99‰. In a plot of δD vs. $\delta^{18}O$ (Fig. 6), quartz samples plot the area between the meteroric water line and primary magmatic water area. It may reflect that the ore-forming fluid is a mixed water of meteoric water and primary magmatic water.

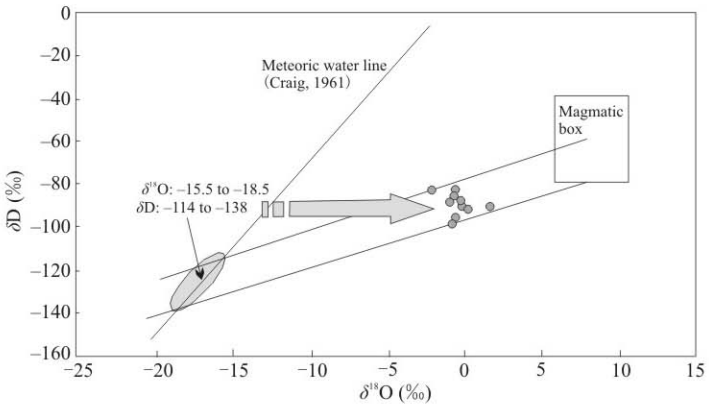

Fig. 6 Hydrogen versus oxygen isotope diagram showing the compositions of hydrothermal fluids for polymetal sulfides quartz veins in the Bianbianshan deposit.
Meteoric water line and primary magmatic water box are taken from Craig (1961).

6 Sulfur and Lead Isotopes

6.1 Sulfur isotopes

All samples were taken from underground tunnels. Sulfides crystals were separated from hand specimens by conventional preparation techniques including crushing, oscillating, heavy liquid and magnetic separator. All mineral separates were further purified by hand-picking under microscope to at least 99% purity. The process and analysis of samples were completed at Institute of Geology and Geophysics, Chinese Academy of Sciences (IGGCAS).

Sulfur isotope compositions of the extracted SO_2 were determined on a Finnigan Mat 252 mass sepectrometer. The $^{34}S/^{32}S$ ratios are expressed by the conventional $\delta^{34}S$ value in ‰ relative to CDT. Reproductivities of $\delta^{34}S$ values are ±0.2‰. The analytical results are given in Table 3.

Table 3 Sulfur isotope compositions of sulfides from the Bianbianshan deposit

Sample No.	Sample description	Location	Minerals	$\delta^{34}S$ (‰)
B3-4	Polymetal sulfides quartz vein	V1, 3level	Py	−0.27
B3-4-1	Polymetal sulfides quartz vein	V1, 3level	Sph	−0.59
B3-8	Polymetal sulfides quartz vein	V1, 3level	Sph	−0.21
B3-11	Polymetal sulfides quartz vein	V1, 3level	Py	0.49
B3-11-1	Polymetal sulfides quartz vein	V1, 3level	Sph	0.08
B4-2	Polymetal sulfides quartz vein	V1, 4level	Py	−1.16
B4-2-1	Polymetal sulfides quartz vein	V1, 4level	Sph	−0.84
B4-16	Polymetal sulfides quartz vein	V4, 4level	Cp	−1.50
B4-16-1	Polymetal sulfides quartz vein	V4, 4level	Sph	−1.22
B5-16	Polymetal sulfides quartz vein	V4, 5level	Sph	−0.34
B5-17	Polymetal sulfides quartz vein	V4, 5level	Cp	−1.11
B5-16-1	Polymetal sulfides quartz vein	V4, 5level	Cp	−0.77
B5-11	Polymetal sulfides quartz vein	V2, 5level	Py	0.48
B5-4	Polymetal sulfides quartz vein	V1, 5level	Ga	−1.67
B5-12	Polymetal sulfides quartz vein	V1, 5level	Sph	0.31
B5-13	Polymetal sulfides quartz vein	V3, 5level	Sph	−0.54
B5-13-1	Polymetal sulfides quartz vein	V3, 5level	Py	0.46

The $\delta^{34}S$ values of 17 sulfide samples from the Bianbianshan deposit vary from –1.67‰ to 0.49‰, with an average value of –0.49‰. The $\delta^{34}S$ values of 5 pyrite samples from ores are concentrated in a narrow range near 0‰, from –1.16‰ to 0.49‰, with an average value of 0.00‰. The $\delta^{34}S$ values of 8 sphalerite samples from ores range from –1.22‰ to 0.31‰, with an average value of –0.44‰. Three chalcopyrite separates of ores have $\delta^{34}S$ values varying from –1.50‰ to –0.77‰, with an average value of –1.13‰, whereas one galena sample from ore has the $\delta^{34}S$ value of –1.67‰. No significant variation in the $\delta^{34}S$ values has been observed from the deposit. The horizontal or vertical zonation of sulfide isotope compositions is not observed.

6.2 Lead isotopes

The process and analysis procedure were seen Zeng et al. (2009a). Isotopic ratios were measured with the VG-354 mass-spectrometer at IGGCAS. Routine analytical precision for standard material was 0.06‰. The 2σ variations are 0.1%, 0.09% and 0.30% for $^{206}Pb/^{204}Pb$,

Table 4 Lead isotope compositions of sulfides from the Bianbianshan deposit

Sample No.	Minerals	Sample location	$^{206}Pb/^{204}Pb$	$^{207}Pb/^{204}Pb$	$^{208}Pb/^{204}Pb$
B3-4	Pyrite	V1, 3level	17.7475	15.5756	37.9322
B4-2	Pyrite	V1, 4level	17.7520	15.6036	38.0030
B4-16	Chalcopyrite	V4, 4level	17.7515	15.6011	37.7064
B4-16-1	Sphalerite	V4, 4level	17.6797	15.5238	37.7423
B5-7	Galena	V2, 5level	17.7320	15.5926	37.9558
B5-16	Sphalerite	V4, 5level	17.6887	15.5230	37.7319
B5-11	Pyrite	V2, 5level	17.6971	15.5468	37.7079
B5-4	Galena	V1, 5level	17.6865	15.5115	37.6863
B5-16-1	Chalcopyrite	V4, 5level	17.6618	15.4960	37.6351

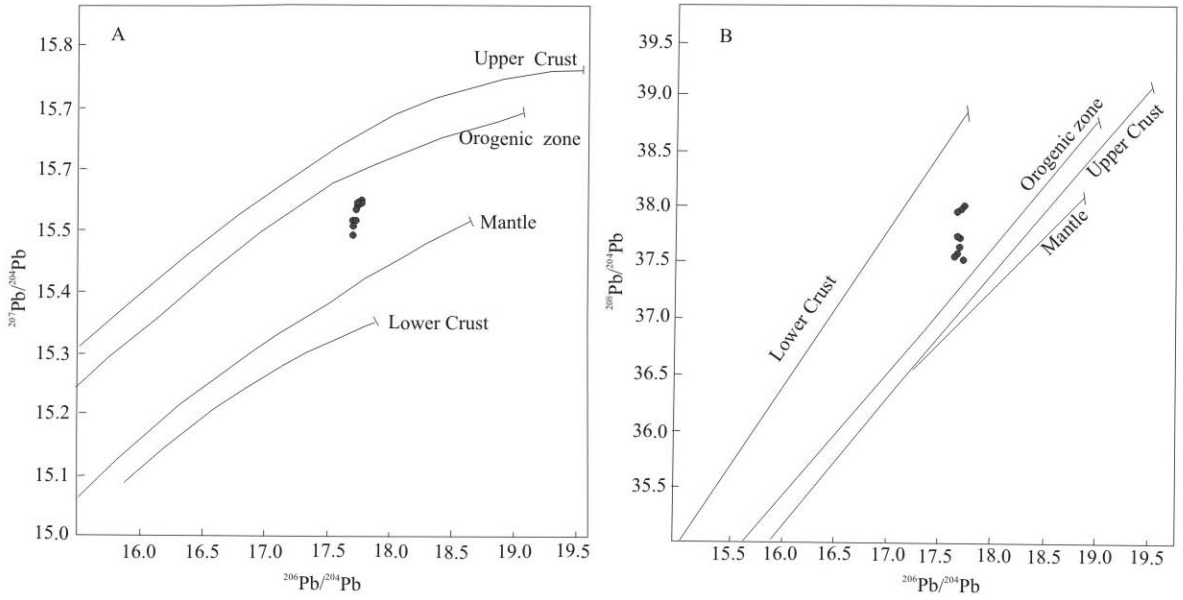

Fig. 7 $^{207}Pb/^{204}Pb$ versus $^{206}Pb/^{204}Pb$ and $^{208}Pb/^{204}Pb$ versus $^{206}Pb/^{204}Pb$ diagram of sulfides from the Bianbianshan deposit.
Lead isotope curves for the upper crust, lower crust, orogen, and mantle are from Zartman and Haines (1988).

$^{207}Pb/^{204}Pb$ and $^{208}Pb/^{204}Pb$ ratios, respectively. The analytical results are presented in Table 4, and Figure 7 shows the plot the lead isotopic ratios. All these sulfide samples have a relatively spread in $^{206}Pb/^{204}Pb$, ranging from 17.6618 to 17.7520, relatively high $^{207}Pb/^{204}Pb$ ranging from 15.4960 to 15.6036, and $^{208}Pb/^{204}Pb$ from 37.6351 to 38.0030.

7 Discussion

7.1 Tectonic setting of the deposits in south segment of the Da Hinggan Mountains and its relationship to magmatism

The Da Hinggan Mountains are mainly composed of Late Paleozoic (principally Permian) metamorphosed volcanic and sedimentary rocks and Jurassic–Cretaceous terrestrial volcanic and sedimentary rocks. The Permian sedimentary rocks show a continuous upward facies change from submarine to terrestrial and a continuous upward decrease in volcanic material as a whole (Liu et al., 2001). Zhang and Zhao (1993) had suggested that during the Permian, the Da Hinggan Mountains were placed in a volcanic arc of active continental margin. Most of metal deposits (except sedimentary exhalative deposits) are related to the magamatic activities and volcanic-subvolcanic activities in Mesozoic (Zhang and Zhao, 1993; Zhang et al., 1994; Zhao and Zhang, 1997; Zeng et al., 2009a), and formed during the late stage of the crust thinning of North China (Mao et al., 2003, 2005; Zhai et al., 2004; Zhang et al., 2011).

The features of the Bianbianshan deposit area suggests that it is related to the Cretaceous volcanic-subvolcanic activity. The ore veins were formed in dilatation space of the fault. The deposit formed during the late stage of the crust thinning of North China. The gold-polymetal mineralization in the Bianbianshan deposit is related to the intrusive dykes, while were emplaced after the volcanic rocks.

7.2 Source of ore-forming fluids

The calculated oxygen isotope composition of fluid varies from –1.98‰ to 1.71‰. The hydrogen isotopic composition measured directly from inclusion fluids, gave a relatively narrow spread between –83‰ and –99‰. In the plot of δD vs. $\delta^{18}O$ (Fig. 6) all samples locate in the area between the meteoric water line and magmatic water

box. This implies that the mixing water fluid may have been dominant at the Bianbianshan deposit.

7.3 Source of ore-forming materials

The isotopic composition of sulfides precipitated from hydrothermal fluid rests with the $\delta^{34}S$ values of source materials, physical and chemical condition during hydrothermal fluid transfer and deposition (Ohmoto, 1972). The average value of $\delta^{34}S$ of minerals can represent that of the total sulfur in the hydrothermal fluid when there are not high fo_2 minerals like hematite in ore deposit (Ohmoto and Rye, 1979). The sulfur-bearing minerals of the Bianbianshan deposit are mainly sulfides (pyrite, sphalerite, galena and chalcopyrite). Therefore, the bulk of the $\delta^{34}S$ values of the Bianbianshan deposit during the main mineralizing stage are restricted to the interval of –1.67‰ –0.49‰, with an average of –0.49‰. This relatively tight clustering can be interpreted to indicate the fluid redox state was below the sulfate / reduced sulfur species boundary, and reduced sulfur species were dominant in the fluids (Ohmoto and Rye, 1979). As shown in Table 3, the $\delta^{34}S$ values of pyrite separated from ores are similar to those of other sulfides from ores. This feature may reflect that that sulfur of pyrite, sphalerite, galena and chalcopyrite from ores could have derived the similar source, and these sulfides deposited from the same hydrothermal activity. The $\delta^{34}S$ values of sulfides from the Bianbianshan deposit are similar to magmatic or igneous sulfide sulfur (Ohmoto and Rye, 1979). The gold-polymetal deposit occurs within the volcanics, and the mineralization and dacite porphyry dike have a close relationship in space and time. These features indicate that sulfur was likely derived from both the magma and volcanic rocks.

As can be seen from the plumbotectonic diagram (Fig. 7) of the Zartman and Haines (1988), the Pb-isotopic data of sulfides samples are plotted in the mantle and orogenic reservoir fields. The line found in data on ores was probably formed through mixing of variable proportions of mantle and orogenic belt lead. The high $^{206}Pb/^{204}Pb$, $^{207}Pb/^{204}Pb$ and $^{208}Pb/^{204}Pb$ ratios in the deposit may reflect a high content of radiogenic Pb in the hydrothermal ore-forming solution. An input of radiogenic lead-bearing material or fluids to the initial Pb-isotope system is possible during the ore-forming processes. There is a paragenetic association between gold and sulfides in the ores, this indicate that both sulfides and gold mineral were precipitated from the same ore-forming fluids. Therefore, the lead source may indicate the source of gold.

7.4 Deposition of ore-forming materials

Gas analyses of fluid inclusion show that the gas compositions are dominating H_2O (>97%), CO_2(<2%), with minor of N_2, CH_4, C_2H_6, H_2S and Ar, the existence of these minor content gases reflect that the mineralization took place in a reducing environment. A large number of factors may cause gold precipitation (Seward, 1973). Many studies show that fluid mixing is the important factor that could cause the physical-chemical condition change of the ore-forming hydrothermal fluid system such as temperature, Ph and Eh (Hofstra et al., 1991). Any change of the geochemical parameters may cause gold precipitation (Hayashi and Ohmoto, 1991; Edward, 1998). In the Bianbianshan deposit, fluid mixing between magmatic fluid and meteoric water may be implicated as an important mechanism for ore deposition as discussed above.

7.5 Metallogeny

Hydrothermal gold-polymetal mineralization in the Bianbianshan deposit is closely related to the volcanic-subvolcanic activity and controlled by structure. The deposit might be formed by coaction of lasting subvolcanic magmatic activity, hydrothermal circulation, fluid mixing, and favored structural setting.

The controlling fault zone within the Cretaceous volcanic rocks, resulted from shear stress, and formed at the late stage of the crust thinning in Cretaceous. Deep-sourced hot fluids associated with subvolcanic activity ascend along faults up to shallow depths, where fluid mixing between the deep hot fluid and the cool meteroric water, as well as water-rock reaction took place. The fluid mixing caused a rapid temperature change, at the same time, the pressure of the ascending fluid dropped down too. These factor changes cause the Au-polymetal deposition in favored structural setting.

8 Conclusions

(1) The Bianbianshan gold-polymetal deposit occurs within the Hercynian fold belt of the south segment of DHMP and is hosted by Cretaceousc andesite and tuff. The distribution of ore bodies is structurally controlled by faults. The faults provided conduits for transport of ore-bearing fluids and favored structural site for ore deposition, especially, the dilatation space of fault.

(2) Mineralization is closely associated with intense hydrothermal alteration mainly controlled by faults, with a typical alteration assemblage of quartz + sericite + chlorite + calcite. These veins were formed at temperatures from 80°C to 360°C

(3) H and O isotopes suggest that the ore-forming fluid of the Bianbianshan gold-polymetal deposit may be a mixture of magmatic water with meteoric water.

(4) Sulfur isotope compositions of sulfides from the ores give $\delta^{34}S$ values close to zero indicating a magmatic source of the sulfur. The lead isotope compositions of sulfides from the ores indicate that lead in ores might be a mixture of variable proportions of mantle and orogenic belt lead.

(5) Gold-polymetal deposit might be formed by coactions of lasting volcanic-subvolcanic magmatic activity, hydrothermal circulation, fluid mixing, and favored structural setting. Fluid mixing might be the key factor controlling ore deposition.

Acknowledgments

This work was financially supported by the National Natural Science Foundation of China (No. 40972065) and the Special Project (No. XDA08100500) of the Chinese Academy of Science. We thank Prof. Zhang, Fusong for H, O and S isotope analyses, and Prof. Zhu Heping for analyses of gases in fluid inclusions.

Manuscript received Jan. 10, 2012
accepted Apr. 16, 2012
edited by Liu Lian

References

Bureau of Geology and Mineral Resources of Neimongol Autonomous Region (BGMR), 1991. *Regional geology of Neimonggol Autonomous Region*. Beijing: Geological Publishing House, 1–532 (in Chinese with English abstract).

Bureau of Geology and Mineral Resources of Neimongol Autonomous Region (BGMR), 1996. Stratigraphy (Lithostratic) of Nei Mengol Autonomous Region. Wuhan: China University of Geosciences Press, 1–244 (in Chinese).

Clayton, R.N., and Mayeda, T.K., 1963. The use of bromine pentafluoride in the extraction of oxygen from oxides and silicates for isotopic analysis. *Geochim.et Cosmochim. Acta*, 27(1): 43–52.

Craig, H., 1961. Isotopic variations in meteric waters. *Science*, 133: 1702–1703.

Edward, J.M., 1998. Hydrothermal transport and depositional processes in Archean lode-gold systems: A review. *Ore Geol. Rev.*, 13(1–5): 307–321.

Hayashi, K., and Ohmoto, H., 1991. Solubility of gold in NaCl and H_2S-bearing aqueous solutions at 250–350°C. *Geochim. et Cosmochim. Acta*, 55(8): 2111–2126.

Hofstra, A.H., Levental, J.S., Northrop, H.P., Landis, G.P., Rye, R.O., Birak, D.L., and Dahl, A.R., 1991. Genesis of sediment-hosted disseminated-gold deposits by fluid mixing and sulfidization: Chemical-reaction-path modeling of re-depositional processes documented in the Jerritt Canyon district, Nevada. *Geology*, 19(1): 36–40.

Li Deting, Zeng Qingdong, Liu Jianming and Liu Hongtao, 2008. Geological features of Silver-Lead-Zinc polymetalliic deposit in Southeast section of Daxinganling- with Lamahan deposit as the case. *Metal Mine*, 385(7): 70–73 (in Chinese with English abstract).

Liu Jianming, Ye Jie, Li Yongbing, Chen Xusong and Zhang Ruibin, 2001. A preliminary study on exhalative mineralization in Permian basins, the southern segment of the Da Hinggan Mountains, China: Case studies of the Huangganglіang and Dajing deposits. *Res. Geol.*, 51(2): 345–358.

Mao Jingwen, Xie Guiqing, Li Xiaofeng, Wang Yitian, Zhang Changqian and Li Yongfeng, 2005. Mesozoic large-scale metallogenic pulses in North China and corresponding geodynamic settings, *Acta Petrologica Sinica*, 21(1): 169–188 (in Chinese with English abstract).

Mao Jingwen, Zhang Zuoheng, Yu Jinjie, Wang Yitian and Niu Baogui, 2003. The geodynamic setting of Mesozoic large-scale mineralization in North China: The revelation from accurate timing of metal deposits. *Science in China* (Series D), 33(4): 289–300 (in Chinese).

Matsuhisa, Y., Goldsmith, J.R., and Clayton, R.N., 1979. Oxygen isotopic fractionation in the system quartz-albite-anorthite-water. *Geochim.et Cosmochim. Acta*, 43(7): 1131–1140.

Ohmoto, H., 1972. Systematics of sulfur and carbon isotopes in hydrothermal ore deposit. *Econ. Geol.*, 67(5): 551– 579.

Ohmoto, H., and Rye, R.O., 1979. *Isotope of sulfur and carbon*. In: Barnes, H.L. (ed.). *Geochemistry of hydrothermal ore deposits*. New York: Wiley, 509–567.

Roedder, E., 1984. Fluid inclusions. *Rev. Mineral.*, 12: 1–64.

Roedder, E., and Bodnar, R.J., 1980. Geologic pressure determinations for fluid inclusion studies. *Ann. Rev. Earth, Planet.Sci.*, 8: 263–301.

Rui Zongyao, Shi Lindao and Fang Ruheng, 1994. *Geology and nonferrous metallic deposits in the northern margin of the North China landmass and its adjacent*. Beijing: Geological Publishing House, 1–476 (in Chinese with English abstract).

Seward, T.M., 1973. Thio complexes of gold and the transport of gold in hydrothermal ore solutions. *Geochem. et Cosmochim. Acta*, 37(3): 379–399.

Shao Jian, 1991, *Crustal evolution in the middle part of the northern margin of the Sino-Korean plate*. Beijing: Peking Univ. Pub. House, 1–144 (in Chinese with English abstract).

Sun Xingguo, 2008. *Metallogenic Model and Prospecting model in Longtoushan Ag-Pb-Zn polymetallic ore deposit, Inner Mongolia.* Beijing: Institute of Geology and Geophysics, Chinese Academy of Sciences (Ph. D thesis): 1–153.

Wang Jingbin, Wang Yuwang and Wang Lijuan, 2000. Copper metallogenic setting and prospecting potential in the middle-southern part of Da Hinggan Mountains. *Geology and Prospecting*, 36 (5): 1–4 (in Chinese with English abstract).

Wu Guang, Chen Yanjing, Sun Fengyue, Zhang Zhe, Liu Ankun and Li Zhitong, 2010. Geochemistry and Genesis of the Late Jurassic Granitoids at Northern Great Hinggan Range: Implications for Exploration. *Acta Geologica Sinica* (English edition), 84(2): 321–332.

Xiao Chengdong, Fu Guoli and Zhao Liqing, 2000. Plate-tectonic evolution and gold deposits, Xilinhaote to north of Chifeng, Inner Mongolia. *Gold Geology*, 6(2): 17–20 (in Chinese with English abstract).

Xiao Chengdong and Yang Zhida, 1997. Two major ore belts north to Chifeng of Inner Mongolia: their geology and Mineralization. *Geological Exploration for Non-ferrous Metals*, 6(4): 197–201 (in Chinese with English abstract).

Zartman, R.E., and Haines, S.M., 1988. The plumbotectonic

model for Pb isotope systematics among major terrestrial reservoirs: A case for bi-directional transport. *Geochim.et Cosmochim. Acta*, 52(6): 1327–1339.

Zeng Qingdong, Liu Jianming, Yu Changming, Ye Jie and Liu Hongtao, 20011a. The metal deposits in the Da Hinggan Mountains, NE China: styles, characteristics, and exploration potential. *International Geology Review*, 53(7), 846–878.

Zeng Qingdong, Liu Jianming, Zhang Zuolun, Chen Weijun and Zhang Weiqing, 2011b. Geology and geochronology of the Xilamulun molybdenum metallogenic belt in eastern Inner Mongolia, China. *International Journal of Earth Sciences*, 100(8): 1791–1809.

Zeng Qingdong, Liu Jianming, Zhang Zuolun, Zhang Weiqing, Chu Shaoxiong, Zhang Song, Wang Zaicong and Duan Xiaoxia, 2011c. Geology, fluid inclusion, and sulfur isotope studies of the Chehugou porphyry molybdenum–copper deposit, Xilamulun metallogenic belt, NE China. *Res. Geol.*, 61(3): 241–258.

Zeng Qingdong, Liu Jianming, Qin Feng and Zhang Zuolun, 2010a. Geochronology of the Xiaodonggou porphyry Mo deposit in northern margin of North China Craton. *Res. Geol.*, 60(2): 192–202.

Zeng Qingdong, Liu Jianming and Zhang Zuolun, 2010b. Re-Os geochronology of porphyry molybdenum deposit in south segment of Da Hinggan Mountains, northeastern China. *Journal of Earth Sciences*, 21(4): 390–401.

Zeng Qingdong, Liu Jianming, Zhang Zuolun, Chen Weijun, Qin Feng, Zhang Ruibin, Yu Wenbin, Zhang Xiaohui and Zhai Mingguo, 2009a. Mineralizing types, geological characteristics and geodynamic background of molybdenum deposits in Xilamulun molybdenum polymetal metallogenic belt on northern margin of North China craton. *Acta Petrologica Sinica*, 25(5): 1225–1238 (in Chinese with English abstract).

Zeng Qingdong, Liu Jianming, Zhang Zuolun, Jia Changshun, Yu Changming, Ye Jie and Liu Hongtao, 2009b. Geology and lead-isotope study of the Baiyinnuoer Zn-Pb-Ag deposit, south segment of the Da Hinggan Mountains, northeastern China. *Resource Geology*, 59(2): 170–180.

Zhai Mengguo, Fan Hongrui, Yang Jinhui and Miao Laicheng, 2004. Large-scale cluster of gold deposits in east Shandong: Anorogenic metallogenesis. *Earth Sci. Frontiers*, 11(1): 81–98 (in Chinese with English abstract).

Zhang Yueqiao, Shi Wei and Dong Shuwen, 2011. Changes of late mesozoic tectonic regimes around the Ordos basin (North China) and their geodynamic implications. *Acta Geologica Sinica* (English edition), 85 (6): 1254–1276.

Zhang Dequan, Ai Xia and Bao Xiupo, 1994. Nonferrous metallic deposits in Huanggang-Ganzhuermiao Mesozoic active region. In: Rui et al. (ed.) Geology and nonferrous metallic deposits in the northern margin of the North China landmass and its adjacent area. *Beijing: Geological Publishing House*, 314–363 (in Chinese).

Zhang Dequan and Zhao Yimingm, 1993. A collection on the Cu-polymetallic deposits in the Da Hinggan Mountains and their adjacent areas. *Beijing: Geological Publishing House*, 1–161 (in Chinese).

Zhao Liqing, Sun Shihua, Xiao Chengdong, Lei Shibin, Mao Qian and Fang Congyi, 2004. Characteristics of gold mineralization in the Erenhot-Ulanhot region, eastern Inner Mongolia. China. *Geology and Resources*, 13(4): 222–228 (in Chinese with English abstract).

Zhao Yiming and Zhang Dequan, 1997. Metallogeny and prospective evaluation of copper-polymetallic deposits in the Da Hinggan Mountains and its adjacent regions. *Beijing: Seismological Press*, 125–144 (in Chinese).